JOURNAL OF AIRCRAFT
Vol. 45, No. 1, January–February 2008

Aeroelastic Response of Composite Helicopter Rotor with Random Material Properties

Senthil Murugan,* Ranjan Ganguli,† and Dineshkumar Harursampath‡
Indian Institute of Science, Bangalore 560 012, India

DOI: 10.2514/1.30180

This study investigates the effect of uncertainty in composite material properties on the cross-sectional stiffness properties, natural frequencies, and aeroelastic responses of a composite helicopter rotor blade. The elastic moduli and Poisson's ratio of the composite material are considered as random variables with a coefficient of variation of around 4%, which was taken from published experimental work. An analytical box beam model is used for evaluating blade cross-sectional properties. Aeroelastic analysis based on finite elements in space and time is used to evaluate the helicopter rotor blade response in forward flight. The stochastic cross-sectional and aeroelastic analyses are carried out with Monte Carlo simulations. It is found that the blade cross-sectional stiffness matrix elements show a coefficient of variation of about 6%. The nonrotating rotor blade natural frequencies show a coefficient of variation of around 3%. The impact of material uncertainty on rotating natural frequencies varies from that on nonrotating blade frequencies because of centrifugal stiffening. The propagation of material uncertainty into aeroelastic response causes large deviations, particularly in the higher-harmonic components that are critical for the accurate prediction of helicopter blade loads and vibration. The numerical results clearly show the need to consider randomness of composite material properties in the helicopter aeroelastic analysis.

Introduction

COMPOSITES are the material of choice for recent aircraft structures because of their superior specific strength and stiffness properties. The nominal material properties of composites used in the structural design process are uncertain because of manufacturing tolerances and lack of precise experimental data [1–6]. Such an imprecision in the material properties can substantially influence the response of aircraft structures [7,8]. The effect of material uncertainties on the aeroelastic response may be exacerbated because of the nonlinearities involved and interactions between the structural and aerodynamic disciplines [9]. Therefore, in the recent years, much work has been done to investigate and quantify the effect of uncertainties on the global response of aircraft structures [10].

A comprehensive survey of uncertainty analysis in aeroelasticity is presented in a recent review paper by Pettit [10]. In the stochastic aeroelastic analysis, uncertainties are considered in the structural, aerodynamic, and control disciplines. In the structural discipline, parameters such as Young's modulus, boundary conditions, geometrical configurations, and loads are considered as random variables and their impact on aeroelastic response is studied. However, all the works on uncertainty analysis in aeroelasticity are related to fixed-wing aircraft [11–13]. In parallel to fixed-wing aircraft, composites are extensively used in the critical structures of rotorcraft. Helicopter rotor blades, which play a dominant role in the overall vehicle performance, are routinely made of composites because of their high strength and stiffness-to-weight ratios and tailorable characteristics [14–18]. Therefore, considerable research has focused on the mathematical modeling of composite rotor blades [19]. However, in addition to the accurate modeling of composite rotor blades, the effect of material uncertainties associated with composites on the helicopter aeroelastic response has to be evaluated. To the best of the authors' knowledge, no work has focused on the effect of material uncertainties on the rotorcraft aeroelastic response. This study focuses on the impact of material uncertainties on the aeroelastic response of a composite helicopter rotor.

For uncertainty analysis, several stochastic methods are available [20–23]. These methods can generally be categorized as intrusive and nonintrusive methods from a computational perspective. The intrusive methods need the governing equations and deterministic analysis programs to be modified to perform uncertainty analysis. In the nonintrusive methods, uncertainty analysis can be performed without any modification of the governing equations or the analysis programs. The governing equations of rotorcraft aeroelasticity are highly nonlinear and fundamentally multidisciplinary. Further, any modification of the rotorcraft analysis programs need domain experts from each discipline [24]. Therefore, the nonintrusive methods can be a good choice for uncertainty analysis of rotorcraft. Monte Carlo

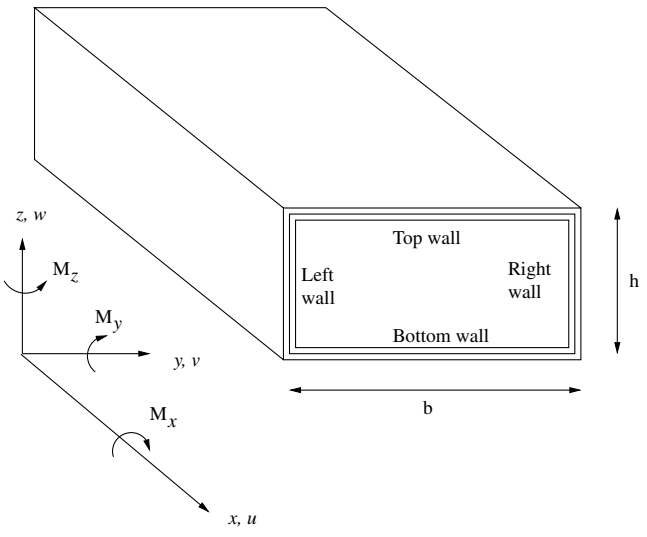

Fig. 1 Composite box beam.

Received 1 February 2007; revision received 5 July 2007; accepted for publication 2 September 2007.

*Graduate Student, Department of Aerospace Engineering; murga@aero.iisc.ernet.in.

†Associate Professor, Department of Aerospace Engineering; ganguli@aero.iisc.ernet.in. Senior Member AIAA.

‡Assistant Professor, Department of Aerospace Engineering; dinesh@aero.iisc.ernet.in. Senior Member AIAA.

Table 1 Baseline hingeless blade properties

Number of blades	4
Radius R, m	4.94
Hover tip speed ΩR, m/s	198.12
Mass per unit length m_o, kg/m	6.46
Lock number	5.2
Solidity	0.07
C_T/σ	0.07
$EI_y/m_o\Omega^2R^4$	0.00834
$EI_z/m_o\Omega^2R^4$	0.02317
$GJ/m_o\Omega^2R^4$	0.00382

Table 2 Stochastic material properties of graphite/epoxy

Material properties	Mean	Coefficient of variation, %	Distribution
E_1, MPa	141.96e3	3.39	Normal
E_2, MPa	9.79e3	4.27	Normal
G_{12}, MPa	6.00e3	4.27	Normal
ν_{12}	0.42	3.65	Normal

simulation (MCS) is the most popular nonintrusive uncertainty analysis technique and can be used without any modification in the existing deterministic analysis programs [1]. With the latest computing machines, computational time for the rotorcraft aeroelastic simulations are acceptable [24]. Therefore, MCS is considered in this study for rotorcraft aeroelastic uncertainty analysis.

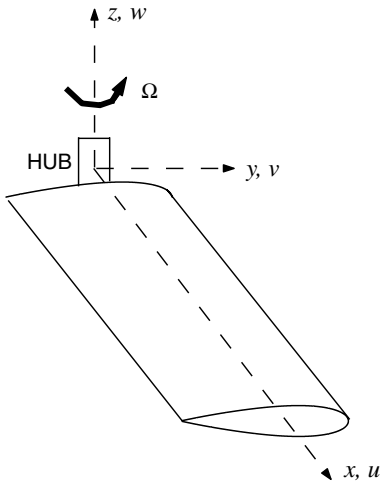

Fig. 2 Elastic rotor blade.

In the current work, the modulus properties E_1, E_2, and G_{12} and Poisson's ratio ν_{12} of composite plies used in the rotor blades are considered as random variables. The rotorcraft uncertainty analysis

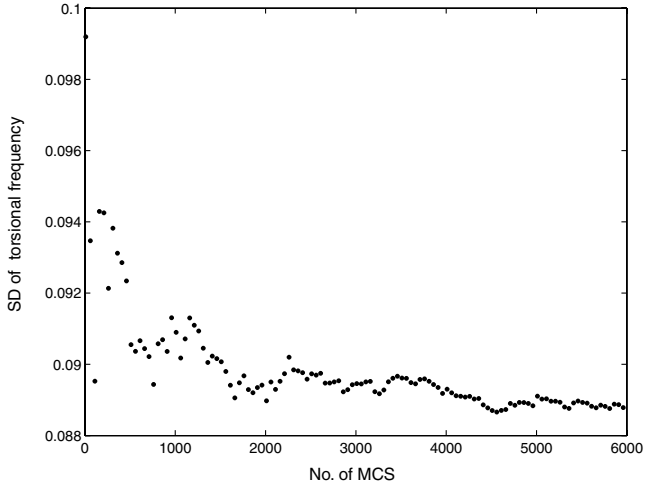

Fig. 3 Convergence of the standard deviation (SD) of torsional frequency.

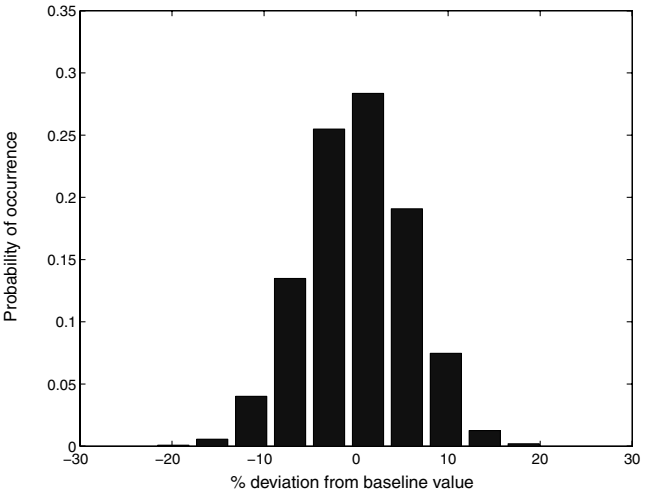

Fig. 4 Probability histogram for torsional stiffness.

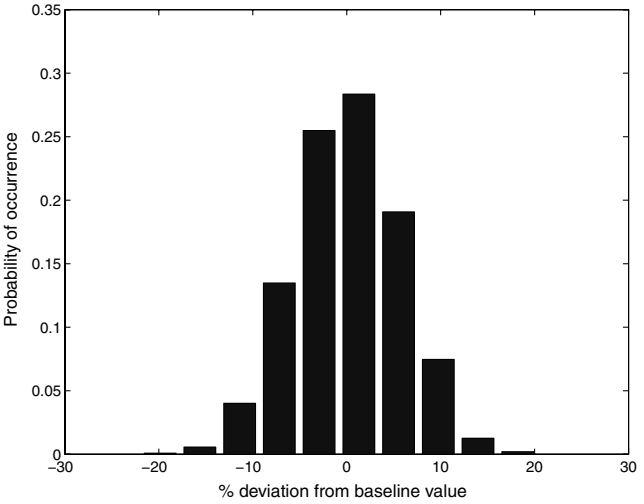

Fig. 5 Probability histogram for flap bending stiffness.

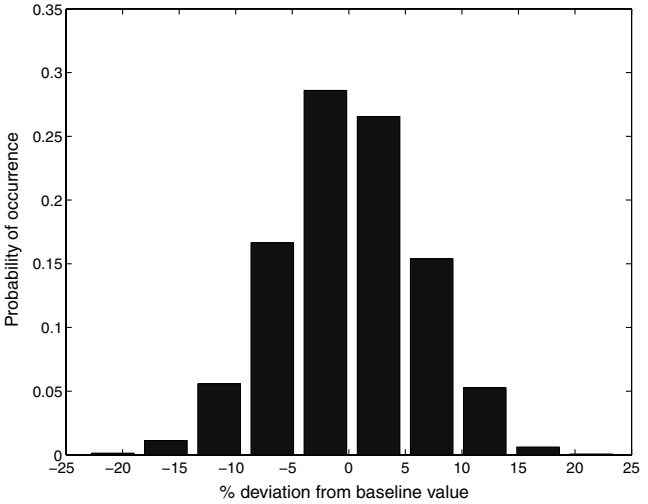

Fig. 6 Probability histogram for lag bending stiffness.

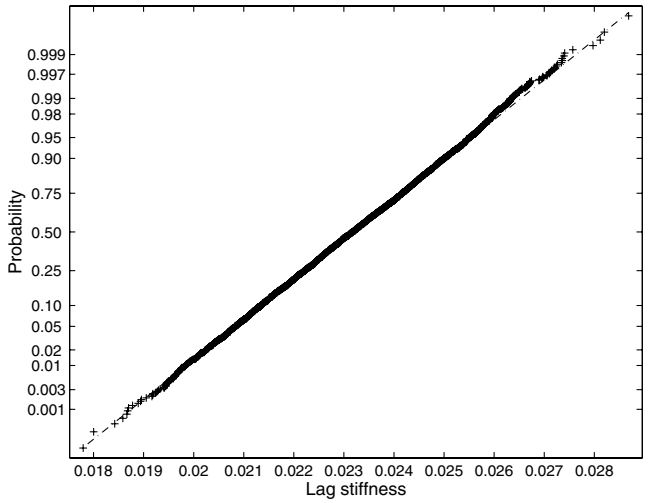

Fig. 7 Normal probability plot for lag bending stiffness.

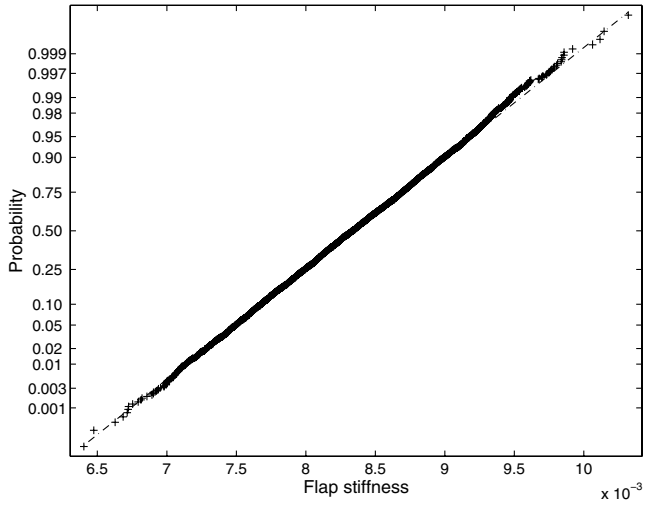

Fig. 8 Normal probability plot for flap bending stiffness.

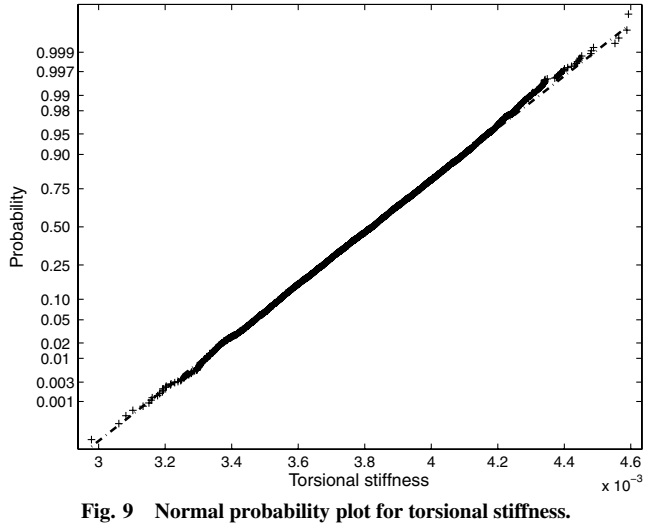

Fig. 9 Normal probability plot for torsional stiffness.

is performed using classical MCS. The uncertainty in the composite material properties is first propagated to the cross-sectional properties of the rotor blade. From the cross-sectional properties, uncertainty is propagated to the free-vibrational characteristics and nonlinear aeroelastic response of the helicopter rotor blade.

Table 3 Statistics of cross-sectional stiffness values

Stiffness	Baseline values, $N \cdot m^2$	Coefficient of variation, %
Flap EI_y	51,580	6.14
Lag EI_z	143,400	6.14
Torsion GJ	23,620	5.60

Rotor Blade Cross-Sectional Analysis

A critical aspect of helicopter rotor dynamic analysis is the calculation of equivalent 1-D beam properties for the 3-D rotor blade. For this purpose, the cross-sectional analysis of composite rotor blade is carried out with analytical models or detailed finite element methods [25,26]. The analytical models have restrictions on the complexity of the blade cross section when compared with the detailed finite element analysis. A composite box beam is generally considered as a good representation of the helicopter blade for preliminary design studies [27]. As an initial effort to quantify the material uncertainty, the helicopter rotor blade is modeled as a thin-walled composite box beam in this study.

A direct analytical formulation presented by Smith and Chopra [27] is used for predicting the effective elastic stiffness of the composite box beam. The analytical formulation has been used for aeroelastic analysis [14] and optimization [28,29] studies and is computationally efficient. The geometry of the composite box beam

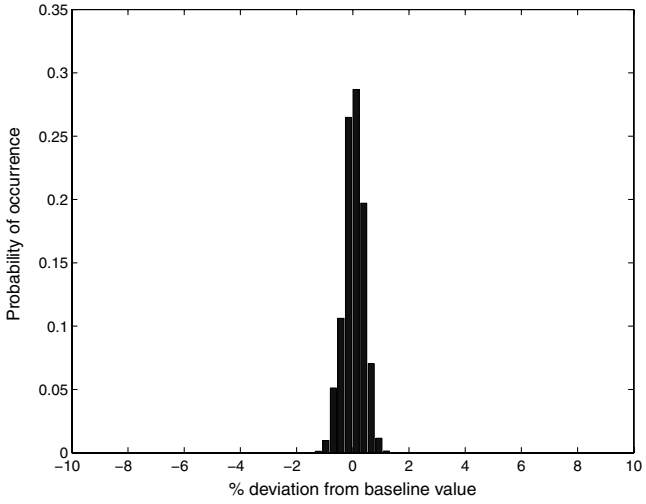

Fig. 10 Probability histogram for fundamental flap frequency.

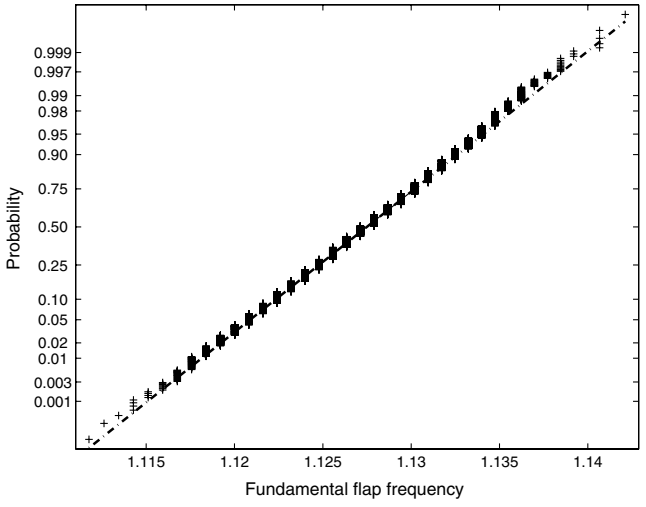

Fig. 11 Normal probability plot for fundamental flap frequency.

Table 4 Statistics of natural frequencies

Mode	Baseline frequencies per revolution (nonrotating blade)	Baseline frequencies per revolution (rotating blade)	Nonrotating blade c.o.v., %	Rotating blade c.o.v., %
Lag 1	0.33	0.71	3.07	2.06
Lag 2	3.49	3.61	3.07	2.68
Lag 3	9.81	10.64	3.07	2.60
Flap 1	0.56	1.12	3.07	0.35
Flap 2	2.09	3.32	3.07	1.23
Flap 3	5.89	7.26	3.07	2.03
Torsion 1	3.54	4.22	2.80	1.26

and the coordinate system used are shown in Fig. 1. The deformation of the box beam is described by three displacements (u, v, and w) and one torsional rotation (ϕ). The cross-sectional stiffness matrix of a composite box beam without initial twist and curvature, built with identical balanced symmetric laminate for all four walls, can be written as in the right-hand side of the relation for general internal forces:

$$\begin{Bmatrix} Q_x \\ M_x \\ -M_y \\ M_z \end{Bmatrix} = \begin{bmatrix} EA & 0 & 0 & 0 \\ 0 & GJ & 0 & 0 \\ 0 & 0 & EI_y & 0 \\ 0 & 0 & 0 & EI_z \end{bmatrix} \begin{Bmatrix} u' \\ \phi' \\ w'' \\ v'' \end{Bmatrix} \tag{1}$$

where Q_x is the axial force; M_x is the torque; M_y and M_x are bending-moment distributions; and EA, GJ, EI_y, and EI_z correspond to equivalent axial, torsional, flap (out-of-plane), and lag (in-plane) bending stiffnesses of the rotor blade. A balanced symmetric laminate is considered because most composite rotor blades today are still conservatively designed to have no couplings, though such couplings can sometimes be useful and/or unavoidable.

Nonlinear Aeroelastic Model

A comprehensive aeroelastic analysis code based on the finite element method is used to evaluate the helicopter blade response. The rotorcraft structure is modeled as a nonlinear representation of composite elastic rotor blades coupled to a rigid fuselage. The

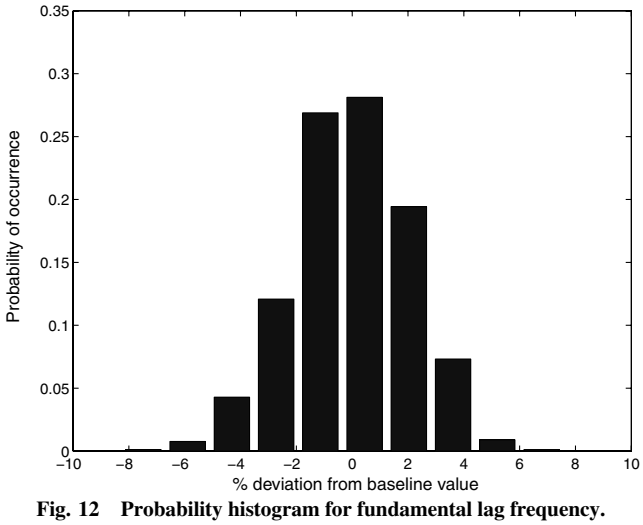

Fig. 12 Probability histogram for fundamental lag frequency.

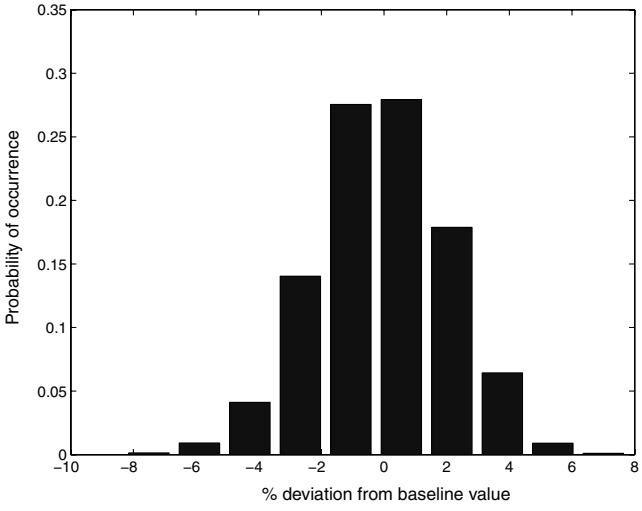

Fig. 14 Probability histogram for fundamental torsional frequency.

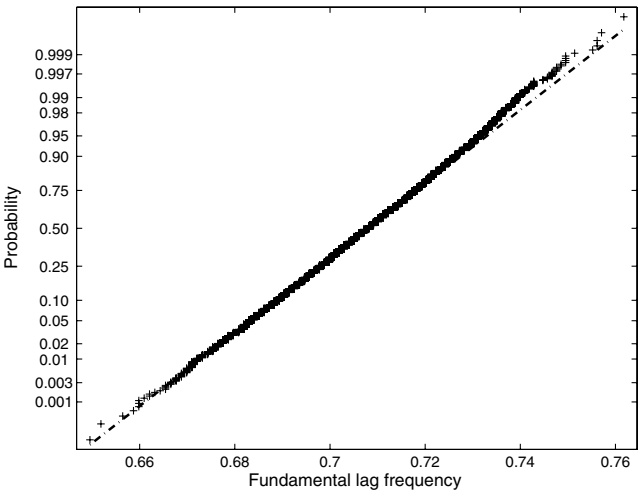

Fig. 13 Normal probability plot for fundamental lag frequency.

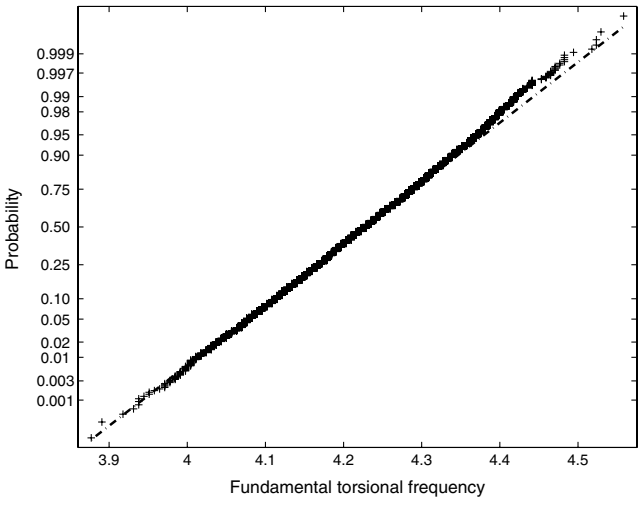

Fig. 15 Normal probability plot for fundamental torsional frequency.

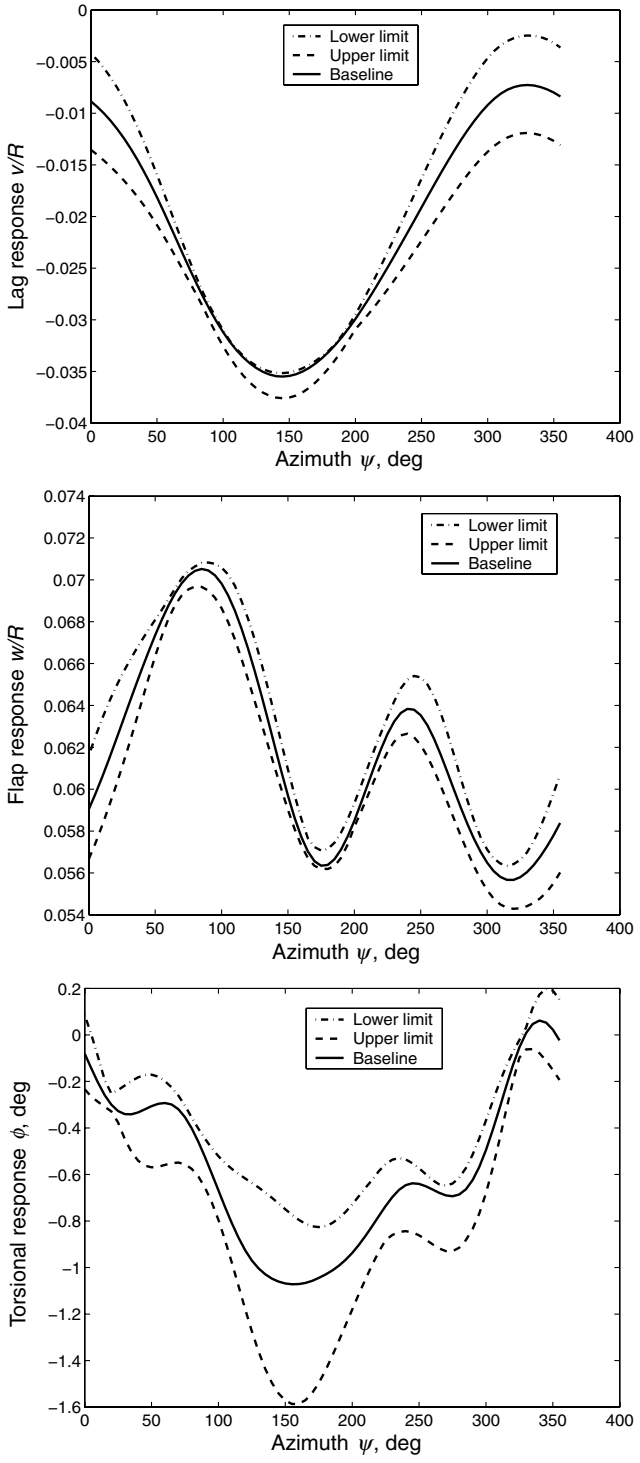

Fig. 16 Effect of uncertainty on blade-tip responses.

rotating elastic rotor blade is modeled as a slender elastic beam undergoing flap bending w, lag bending v, elastic twist ϕ, and axial deflection u, with a rotational speed of Ω, as shown in Fig. 2. The effect of moderate deflections is included by retaining second-order nonlinear terms. Governing equations are derived using a generalized Hamilton's principle applicable to nonconservative systems:

$$\int_{\psi_1}^{\psi_2} (\delta U - \delta T - \delta W)\, \mathrm{d}\psi = 0 \tag{2}$$

where δU and δT are the virtual strain energy and the kinetic energy contributions, respectively, from the elastic blade; δW is the virtual

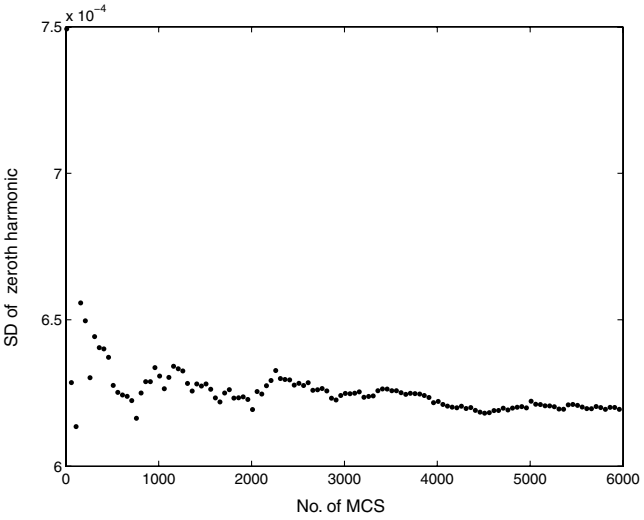

Fig. 17 Convergence of the blade torsion motion for zeroth harmonic a_0.

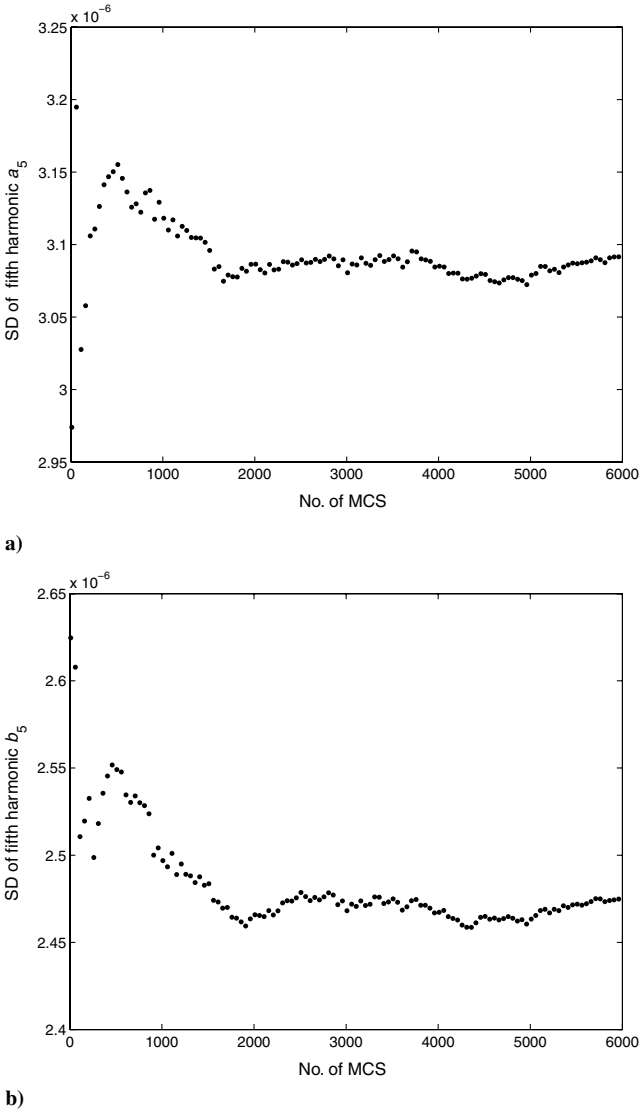

Fig. 18 Convergence of the blade torsion motion.

work done by the external aerodynamic forces acting on the blade; and $\psi = \Omega t$ is the azimuth angle around the rotor disk. The unsteady aerodynamics and free-wake models are used to calculate the aerodynamic forces [30]. The blade is discretized into beam finite

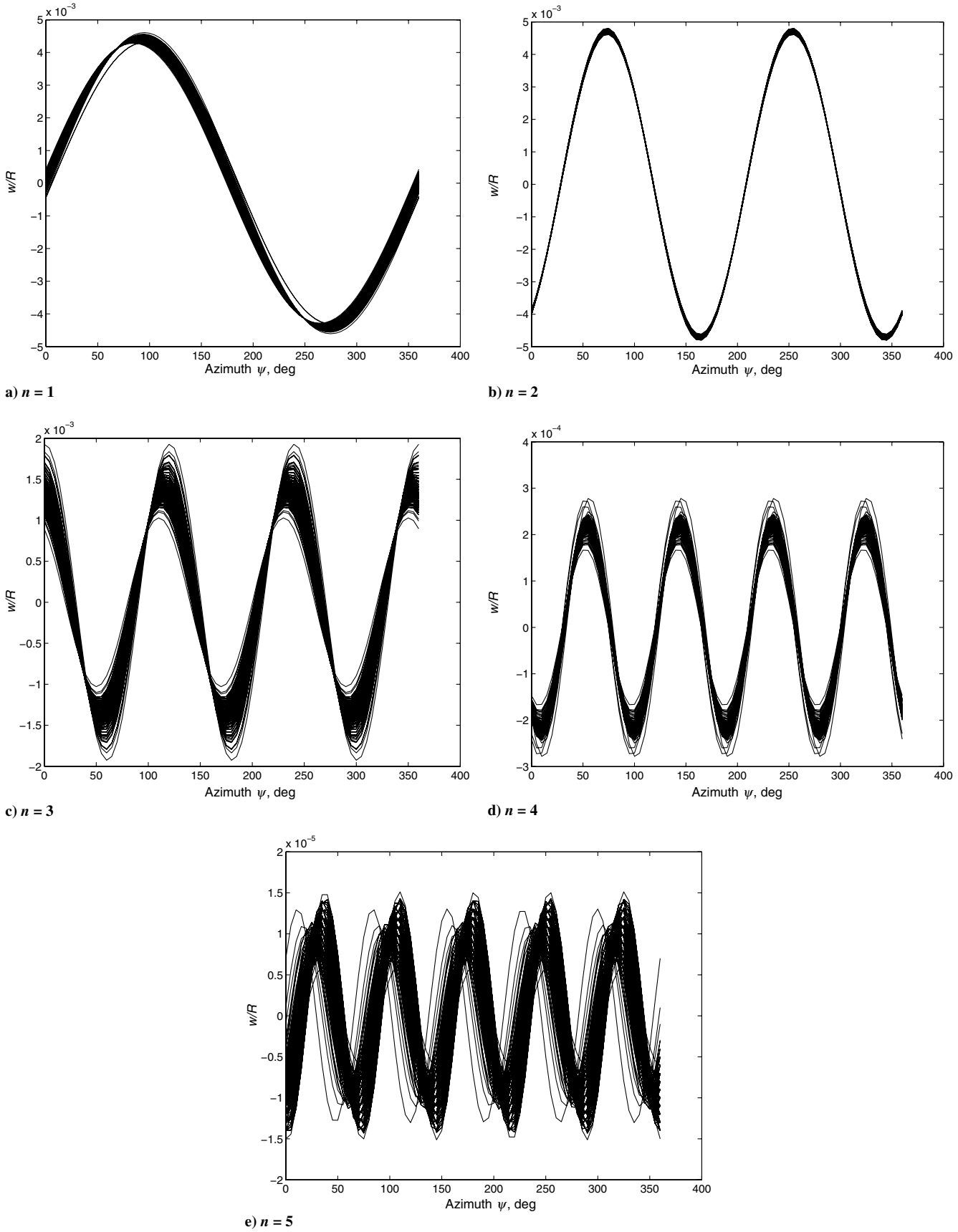

a) $n = 1$ **b) $n = 2$**

c) $n = 3$ **d) $n = 4$**

e) $n = 5$

Fig. 19 Effect of uncertainty on the first five harmonics of the blade-tip flap (out-of-plane bending) response.

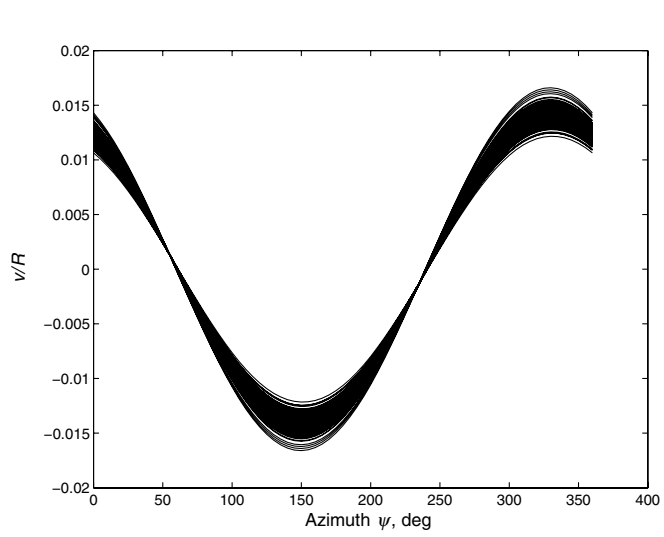

a) $n = 1$

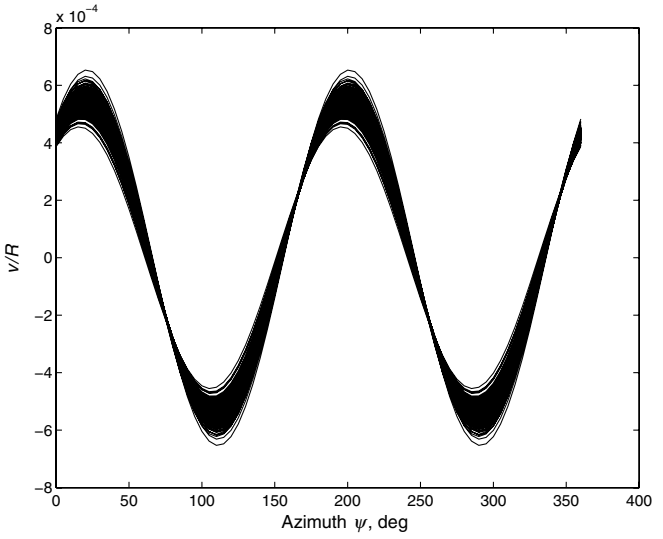

b) $n = 2$

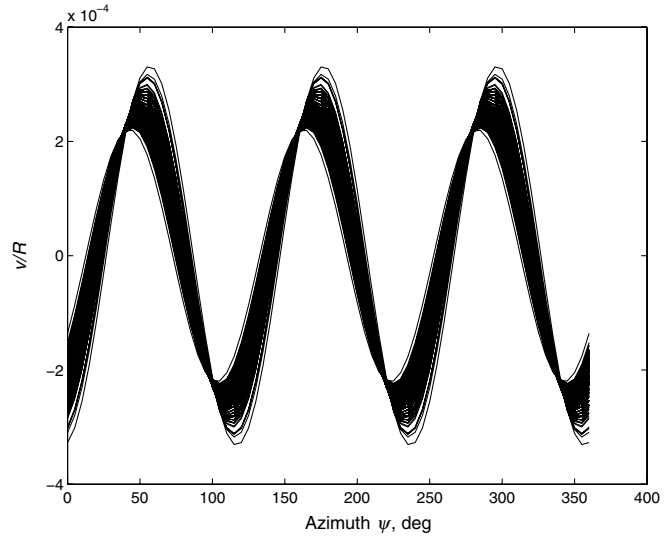

c) $n = 3$

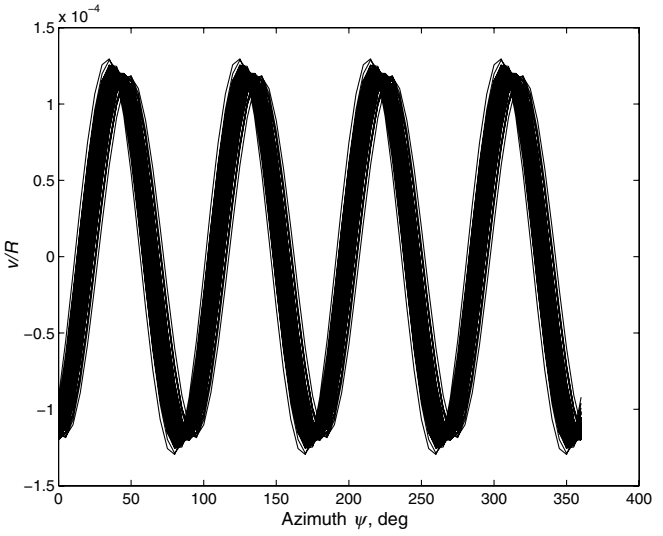

d) $n = 4$

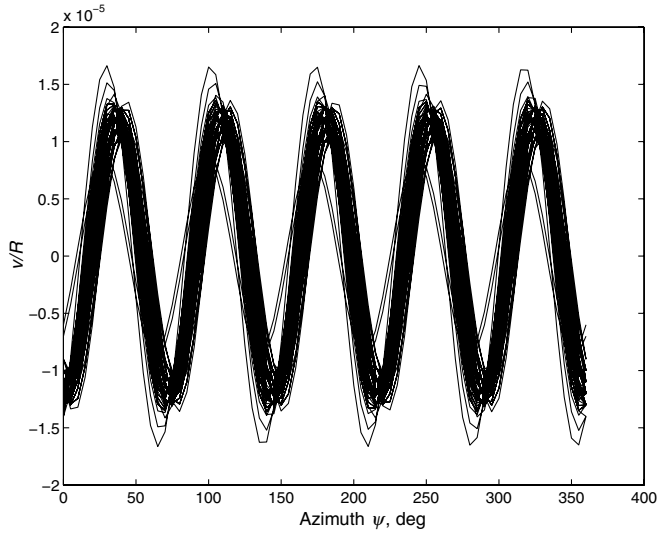

e) $n = 5$

Fig. 20 Effect of uncertainty on the first five harmonics of the blade-tip lag (in-plane bending) response.

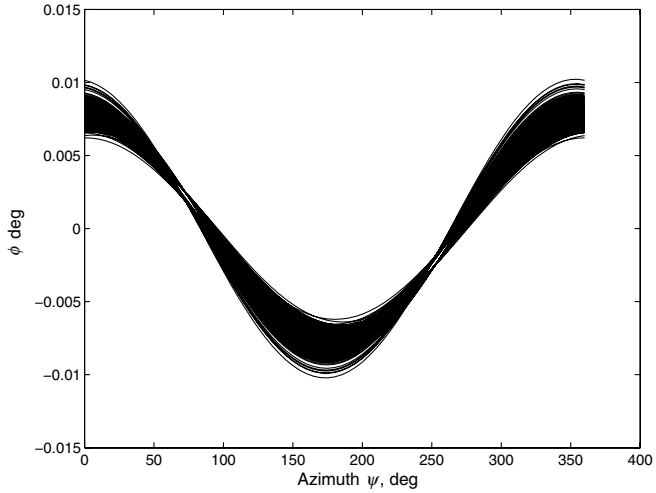

a) $n = 1$

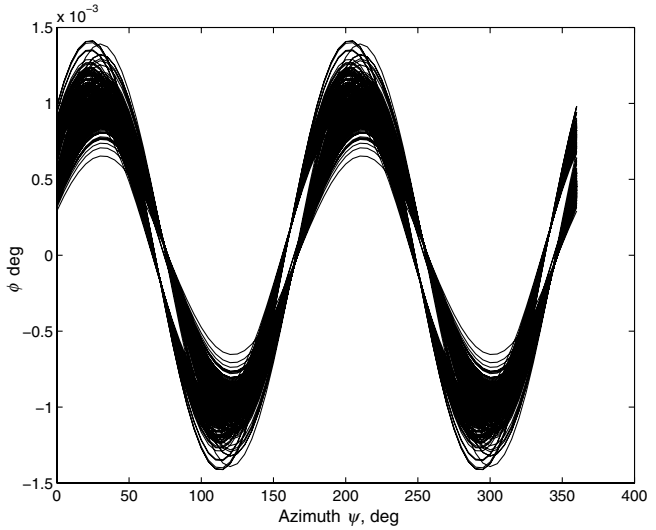

b) $n = 2$

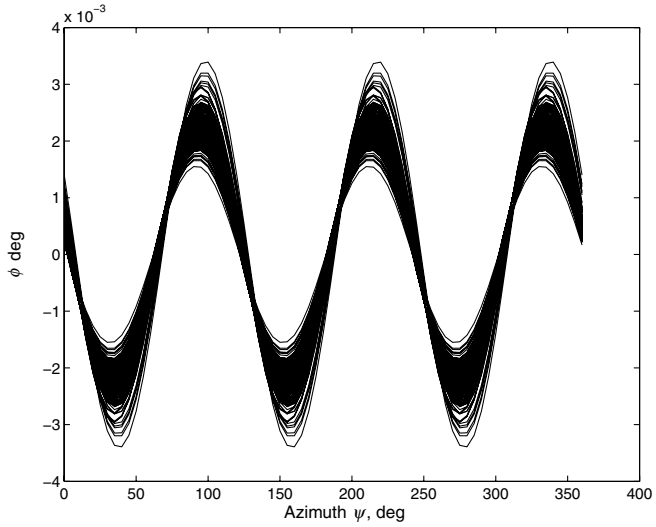

c) $n = 3$

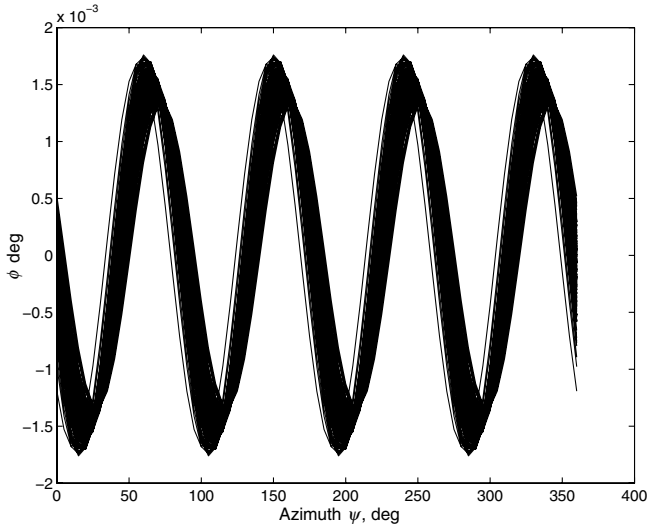

d) $n = 4$

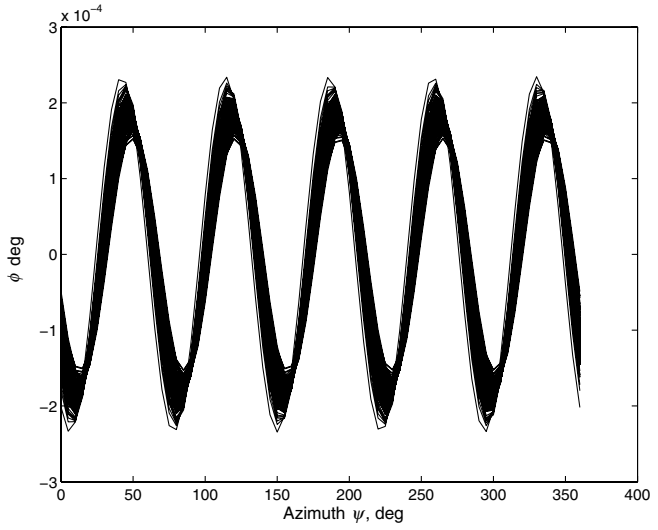

e) $n = 5$

Fig. 21 Effect of uncertainty on the first five harmonics of the blade-tip torsion response.

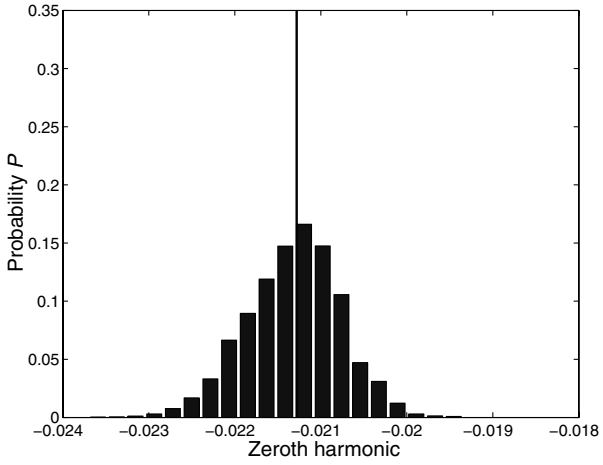

a) Lag

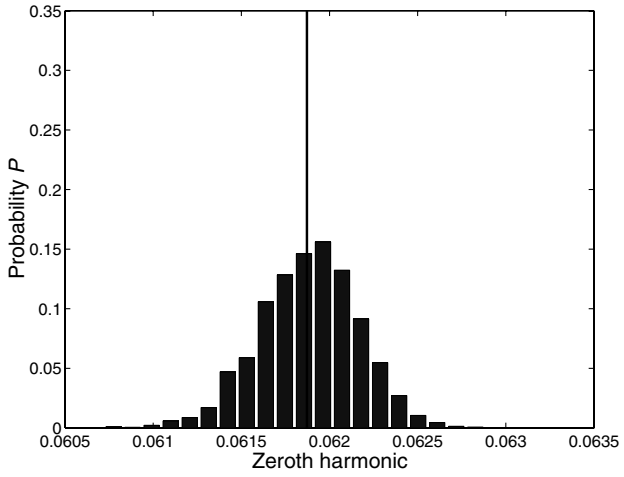

b) Flap

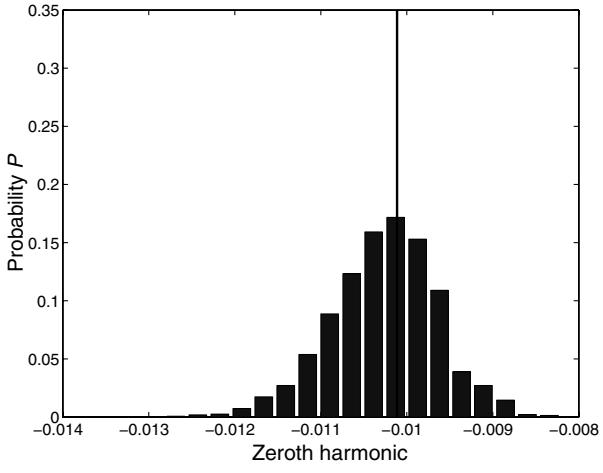

c) Torsion

Fig. 22 Zeroth harmonic of the blade-tip response.

elements, each with 15 degrees of freedom. These degrees of freedom correspond to cubic variations in elastic axial and bending (flap and lag) deflections and quadratic variation in elastic torsion. The finite element equations are reduced in size by using normal-mode transformation. This results in the nonlinear ordinary differential equation with periodic coefficients, as given next:

$$\mathbf{M}\,\ddot{\mathbf{p}}(\psi) + \mathbf{C}\dot{\mathbf{p}}(\psi) + \mathbf{K}\mathbf{p}(\psi) = \mathbf{F}(\mathbf{p}, \dot{\mathbf{p}}, \psi) \tag{3}$$

where $\mathbf{M}$, $\mathbf{C}$, $\mathbf{K}$, $\mathbf{F}$, and $\mathbf{p}$ represent the finite element mass matrix, damping matrix, structural stiffness matrix, finite element force vector, and modal displacement vector, respectively. Nonlinearities in the model occur due to Coriolis terms and moderate deflection assumptions in the strain-displacement relations. These equations are then solved using finite element in time [31] in combination with the Newton–Raphson method [32]. The preceding equations govern the dynamics of the rotor blade. The solutions to the equations are then used to calculate rotor blade loads using the force summation method, in which aerodynamic forces are added to the inertial forces. The blade loads are integrated over the blade length and transformed to the fixed frame to get hub loads. The steady hub loads are used to obtain the forces acting on the rotor and combined with fuselage and tail rotor forces to obtain the helicopter rotor trim equations:

$$\mathcal{F}(\Theta) = \mathbf{0} \tag{4}$$

where Θ are the state variables. These nonlinear trim equations are also solved using the Newton–Raphson method. The helicopter rotor trim equations and the blade-response equations in (3) and (4) are solved simultaneously to obtain the blade steady response and hub loads. This coupled trim procedure is important for capturing the aeroelastic interaction between the aerodynamic forces and the blade deformations. Further details of the analysis are available in [30,33].

Numerical Results

In this section, the effect of material uncertainties on the cross-sectional stiffness, natural frequencies of the nonrotating and rotating blades, and aeroelastic response of the composite rotor blade are studied. The aim of this study is to show the effect of material uncertainty on the aeroelastic analysis predictions rather than calculating the actual mean and higher-order statistical moments of the response. Therefore, a baseline analysis is carried out initially with the mean values of material properties, and the results from nondeterministic analysis are compared with these baseline results.

The rotor blade considered in this study is a uniform blade equivalent to the BO-105 rotor blade [34]. The composite box beam dimensions and ply angles are chosen to match with the BO-105 rotor blade cross-sectional characteristics given in Table 1. The composite box beam has a breadth of 0.144 m, height of 0.081 m, and ply orientation of $[0_3/(+15/-15)_3/(+45/-45)_2]_s$. Each wall of the box beam therefore has 26 plies and each ply is 0.127 mm thick. The composite plies are considered to be made of graphite/epoxy material [27].

Stochastic Cross-Sectional Stiffness Values

Here, the impact of material uncertainty on the box beam cross-sectional stiffness is evaluated. Most of the studies on uncertainty analysis of composite structures generally consider E_1, E_2, G_{12} and ν_{12} as statistically independent random variables and assume a coefficient of variation (c.o.v.) of 5 to 10% for each of these properties [3–6]. Experimental results for scattering in E_1, E_2, and ν_{12} of a graphite/epoxy composite material and their possible distributions are given in [1]. For the present study, E_1, E_2, and ν_{12} are assumed to have Gaussian distributions, and c.o.v. for these parameters are taken from [1]. For G_{12}, the distribution is assumed to be similar to the E_2 distribution, except for the mean value shift, as considered in the literature [2]. With these assumptions, the stochastic material properties of graphite/epoxy are given in Table 2.

The composite box beam stiffnesses are evaluated with the baseline and nondeterministic values of the material properties (Table 2) using MCS. The torsional, flap, and lag bending stiffnesses play a major role in the aeroelastic response. Therefore, the statistical properties of these three cross-sectional stiffness parameters are evaluated with a total of 6000 realizations. The number of realizations is selected based on a convergence study. For example, the convergence of standard deviation (SD) of fundamental torsional frequency is shown in Fig. 3.

The histogram for three stiffnesses (flap, lag, and torsion) are given in Figs. 4–6. All three stiffnesses show normal distributions that are

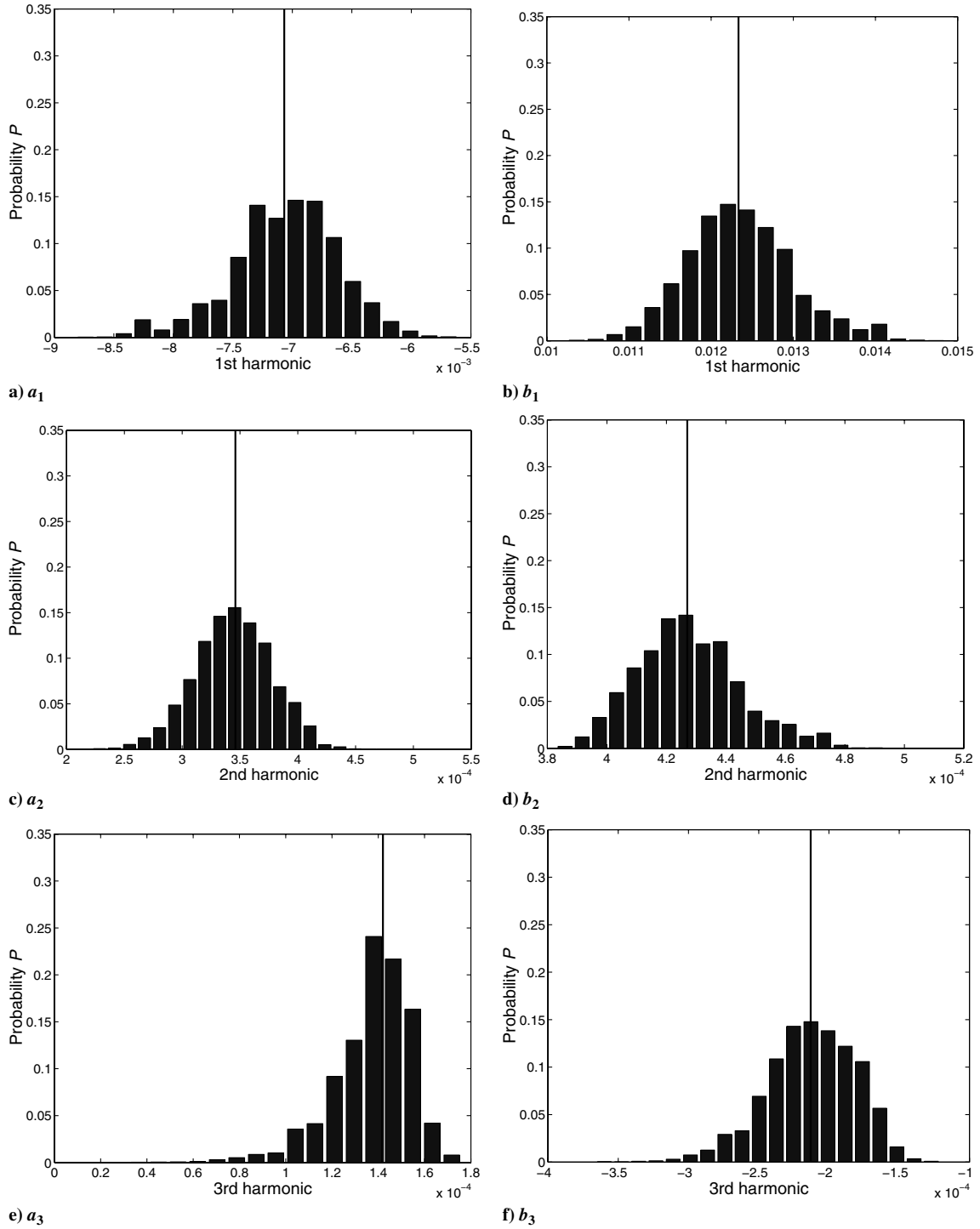

Fig. 23 Probability histogram of the first three harmonics of the blade-tip lag response (solid line is the baseline value).

verified with the normal probability plots shown in Figs. 7–9. The flap and lag bending stiffnesses show similar distributions, whereas the torsional stiffness distribution differs. The distributions typically range between $\pm 20\%$ around the mean stiffness values. The stiffness values and c.o.v. are given in Table 3. The flap, lag, and torsion stiffnesses show a c.o.v. of 6.14, 6.14, and 5.60%, respectively. The flap and lag stiffnesses show similar c.o.v. because in the mathematical modeling of the composite box beam used here [27], flap and lag bending stiffnesses show similar dependencies on the laminate stiffness terms $\bar{Q}_{11}$ and $\bar{Q}_{12}$, whereas the torsional stiffness depends on $\bar{Q}_{26}$ and $\bar{Q}_{66}$, which in turn depend on G_{12}. Furthermore, the four walls of the composite box beam are considered to have the same laminate properties.

Stochastic Natural Frequencies

The stochastic stiffness values calculated in the previous section are used to evaluate the stochastic nonrotating and rotating natural frequencies of the composite rotor blade. The natural frequencies of the nonrotating and rotating blades are calculated by solving the following eigenvalue problem:

$$\mathbf{K}\,\Phi = \omega^2 \mathbf{M}\Phi \tag{5}$$

where the stiffness $\mathbf{K}$ includes the structural stiffness and centrifugal stiffening effect when the blade is rotating, $\mathbf{M}$ is the structural mass matrix, ω are the natural frequencies, and Φ is the vector of degrees of freedom that contains the mode shapes.

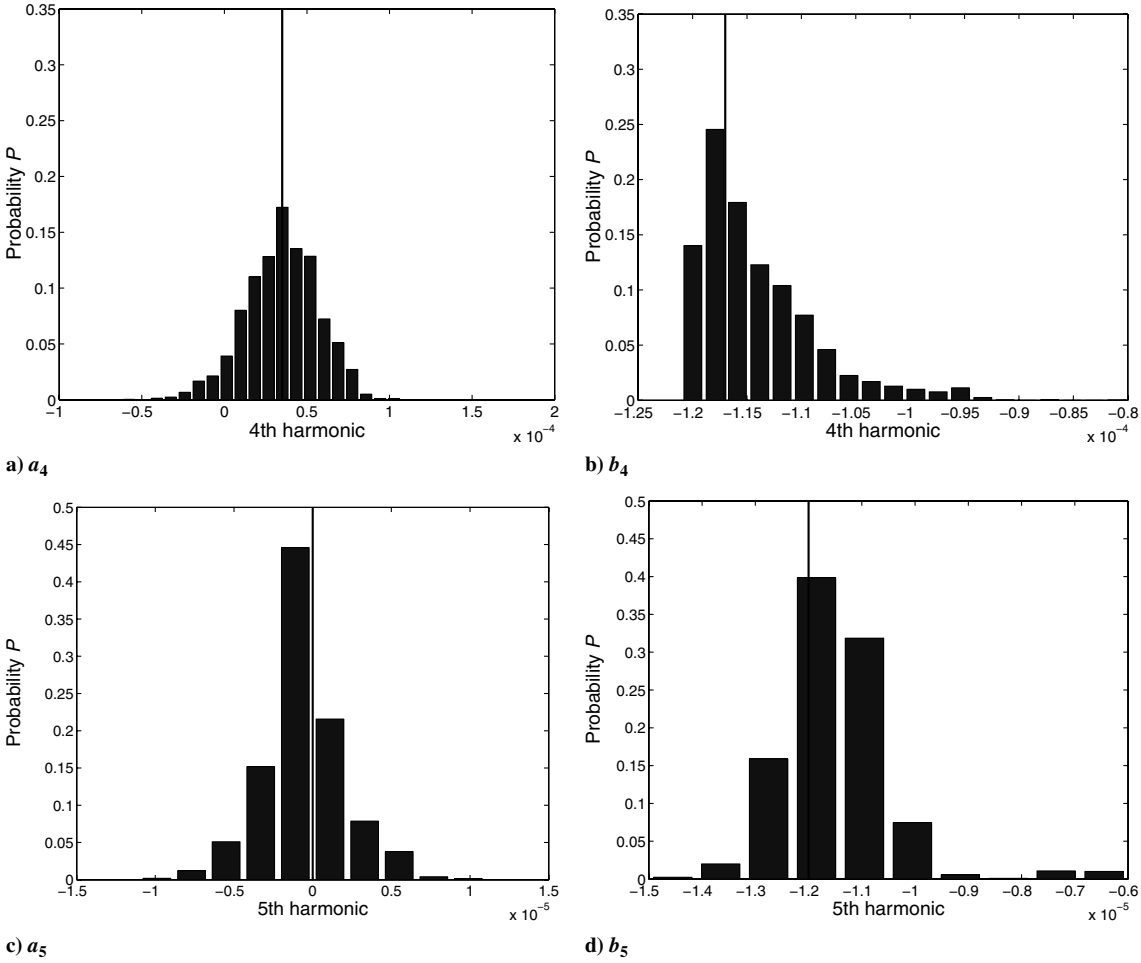

Fig. 24 Probability histogram of fourth and fifth harmonics of the blade-tip lag response (solid line is the baseline value).

For the rotorcraft aeroelastic analysis, three normal modes for lag motion, three normal modes for flap motion, and one normal mode for torsional motion are used to capture the essential dynamics of the system. Therefore, the effect of uncertainties on the corresponding natural frequencies of nonrotating and rotating blades are studied using 6000 MCS. The baseline natural frequencies and c.o.v. of the nonrotating and rotating blades are given in Table 4. The nonrotating blade shows a c.o.v. of 3.07% for the flap and lag bending frequencies and 2.80% for the torsional frequency. The c.o.v. of the nonrotating blade frequencies are half the value of the c.o.v. of the corresponding stiffness values given in Table 3. This is expected, because the mass is assumed deterministic and the nonrotating blade frequencies are proportional to the square root of the corresponding stiffness values.

In contrast to the nonrotating blade, the c.o.v. of the rotating blade frequencies vary with respect to the modes. Among the flap, lag, and torsional fundamental frequencies of the rotating blade, the lag frequency exhibits the highest c.o.v. The histograms and normal probability plots for flap, lag, and torsional fundamental frequencies of the rotating blade are shown in Figs. 10–15. The fundamental lag and torsional frequencies vary $\pm 8\%$ around their baseline values, whereas the fundamental flap frequencies vary just $\pm 1\%$, as explained next.

From Table 4, it is observed that the impact of material uncertainties on natural frequencies of the nonrotating and rotating blades differs in two ways. First, the c.o.v. of rotating blade frequencies are less than the corresponding nonrotating blade frequencies. This difference in the c.o.v. can be explained as follows. In the nonrotating case, blade natural frequencies depend on the square root of the structural stiffness. Therefore, randomness in the structural stiffness expressed as a c.o.v. is halved in terms of the frequencies. For the rotating blade, the natural frequencies depends on the structural stiffness and centrifugal stiffness [35]. Therefore, randomness in the structural stiffness has comparatively less impact on the rotating blade natural frequencies. Second, the c.o.v. of rotating blade frequencies varies with respect to the modes. This is because the centrifugal stiffening has different impacts on the flap, lag, and torsional motions of the rotating blade. For a hingeless rotor blade with uniform mass, the strain energy U can be given as in the Appendix. The strain energy U has contributions from the structural and centrifugal stiffness. The centrifugal stiffness dominates the flap motion of the rotating blade compared with its structural stiffness. For the lag motion, the structural stiffness dominates the motion compared with the centrifugal stiffness. Therefore, the effect of uncertainty in the structural stiffness has a greater influence on the lag frequencies compared with the flap frequencies, as shown in Table 4. For the torsional motion, the structural stiffness is comparatively higher than the centrifugal stiffness and therefore the scattering of the torsional stiffness has a higher impact on its frequency.

Stochastic Aeroelastic Response

In this section, the impact of material uncertainties on the aeroelastic response of the composite helicopter rotor is studied. The aeroelastic response is evaluated with the stochastic beam stiffness values calculated in the earlier section.

The steady-state response of a helicopter blade rotating at speed Ω is periodic, with a period of 2π in a dimensionless time scale, $\psi = \Omega t$ [35]. Therefore, the aeroelastic response of the helicopter blade can be represented as a Fourier series, as given next:

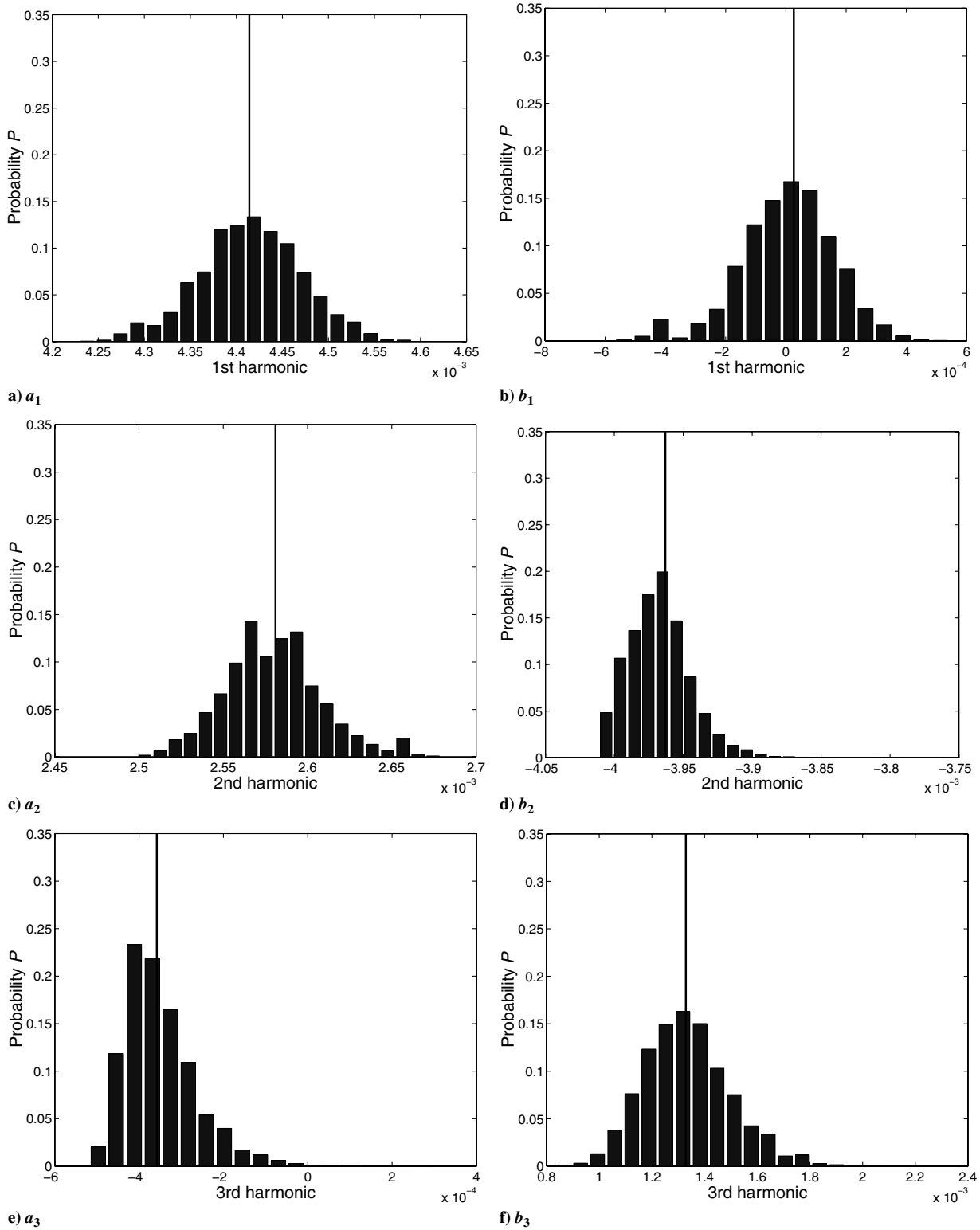

Fig. 25 Probability histogram of first three harmonics of the blade-tip flap response (solid line is the baseline value).

$$\beta(\psi) = a_o + \sum_{n=1}^{\infty}[a_n \sin(n\psi) + b_n \cos(n\psi)] \tag{6}$$

where the response $\beta(\psi)$ represents flap, lag, or torsional motion of the blade. The Fourier coefficients or harmonics a_n and b_n represent the motion of the rotor as a whole. For the four-bladed rotor considered in this study, the first five harmonics (i.e., $n = 1$ to 5) are considered sufficient for accurately representing the rotor motion. The zeroth harmonic a_0 represents the collective motion of the rotor. The first and second harmonics (i.e., a_1, b_1, a_2, and b_2) of the blade response are primarily responsible for dynamic stresses on the blade root of a hingeless rotor. The third, fourth, and fifth harmonics of the blade motion are related to vibratory loads transmitted to the helicopter fuselage. The structural and aerodynamic nonlinearities and higher-order terms play a major role in the prediction of the higher harmonics.

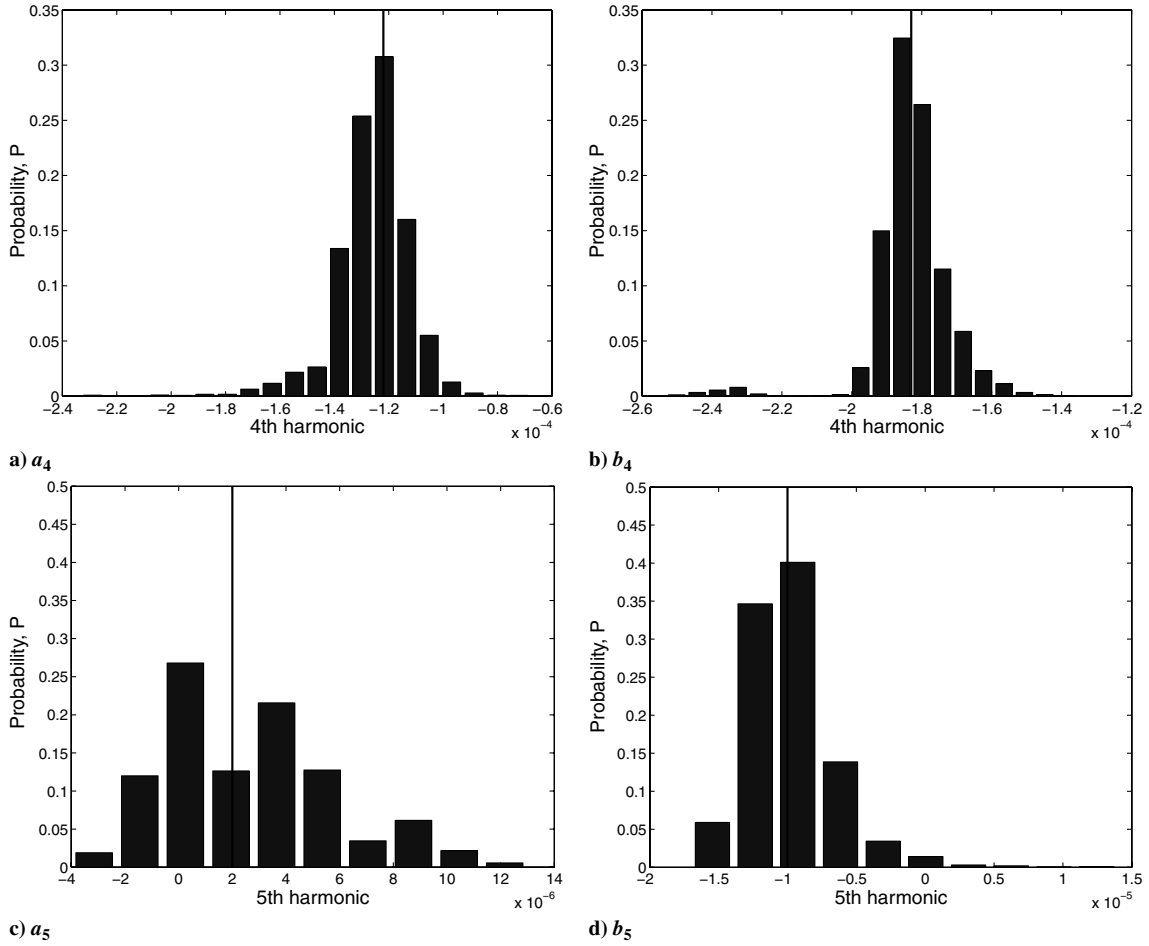

Fig. 26 Probability histogram of fourth and fifth harmonics of the blade-tip flap response (solid line is the baseline value).

The baseline and nondeterministic aeroelastic responses of the composite rotor blade are evaluated with a rotorcraft aeroelastic analysis code [30]. The baseline blade-tip response for flap, lag, and torsional motions for one rotor revolution (i.e., $\psi = 0$ to 360 deg) at an advance ratio of 0.3 are shown in Fig. 16. The stochastic aeroelastic analysis is carried out for stochastic stiffness values evaluated in an earlier section. It is found that the harmonic response converges at 6000 MCS. For example, the convergence of the zeroth and fifth harmonics of the torsion response is shown in Figs. 17 and 18.

The upper and lower limits of the blade-tip response for one rotor revolution from 6000 MCS are given in Fig. 16. At each azimuth, the upper and lower limits of the blade-tip response come from different realizations. Both the flap and lag responses suffer from substantial effects of material uncertainty. The torsional response is the worst affected, with much larger deviations from the baseline value. The scattering of the torsional response is higher in the region of azimuth value of 90 to 270 deg than in other regions. The larger impact of material uncertainty on torsional response is a very important observation because the elastic twist is critical for aeroelastic effects on the rotor blade as well as for the stability and control of the helicopter as a whole.

Truncating the infinite series in Eq. (6), the blade responses can be given as five harmonics, and each harmonic is responsible for accurate prediction of parameters such as vibratory loads or dynamic stresses on the blade root. Therefore, the harmonics of the response are also studied individually. The first five harmonics of flap, lag, and torsional responses are shown in Figs. 19–21, respectively. In the flap response, the first two harmonics are less sensitive to material uncertainty. The magnitudes and phases of the third, fourth, and fifth harmonics of flap response are highly perturbed due to material uncertainty. On the other hand, the magnitudes of even the first two harmonics of lag response show deviations from their baseline values. The third, fourth, and fifth harmonics of lag response show relatively larger deviations in both the magnitude and phase. In contrast to the flap and lag responses, the first two harmonics of torsional response show large scattering in their magnitudes. Similar to the flap and lag responses, the third, fourth, and fifth of the torsional response harmonics also show considerable scattering from their baseline values. In general, it can be observed that the composite material uncertainty has a significant effect on the harmonics of aeroelastic response.

Figures 19–21 show the significant harmonics of the blade response and give a visual indication of the effect of uncertainty. However, the probability distribution of response varies with the azimuth value and can be better quantified by histograms of Fourier coefficients a_n and b_n, which are shown in Figs. 22–28. The zeroth harmonic for flap, lag, and torsion responses are shown in Fig. 22. As an illustration, the normal probability plots for the zeroth harmonic and fourth harmonics of torsional response are shown in Figs. 29–31.

It was observed from results that the Gaussian distribution in composite material properties leads to Gaussian distribution in blade cross-sectional stiffness. More important, the uncertainties in material properties lead to considerably larger and nontrivial uncertainties on the helicopter aeroelastic response. Therefore, the effect of material uncertainty on aeroelastic response needs to be considered for computational prediction and design studies of composite rotor blades. Unmodeled uncertainties may be one of the reasons behind the poor predictions of rotorcraft aeroelastic response that has been observed in many studies [36–39].

The current paper shows that the uncertainty in material properties has considerable effect on helicopter rotor blade aeroelastic predictions. However, it should be pointed out that the extreme values are events with low but finite probability. The results can also change if different c.o.v. values are used. Also, the impact of uncertainty in aerodynamic parameters may be even more than that

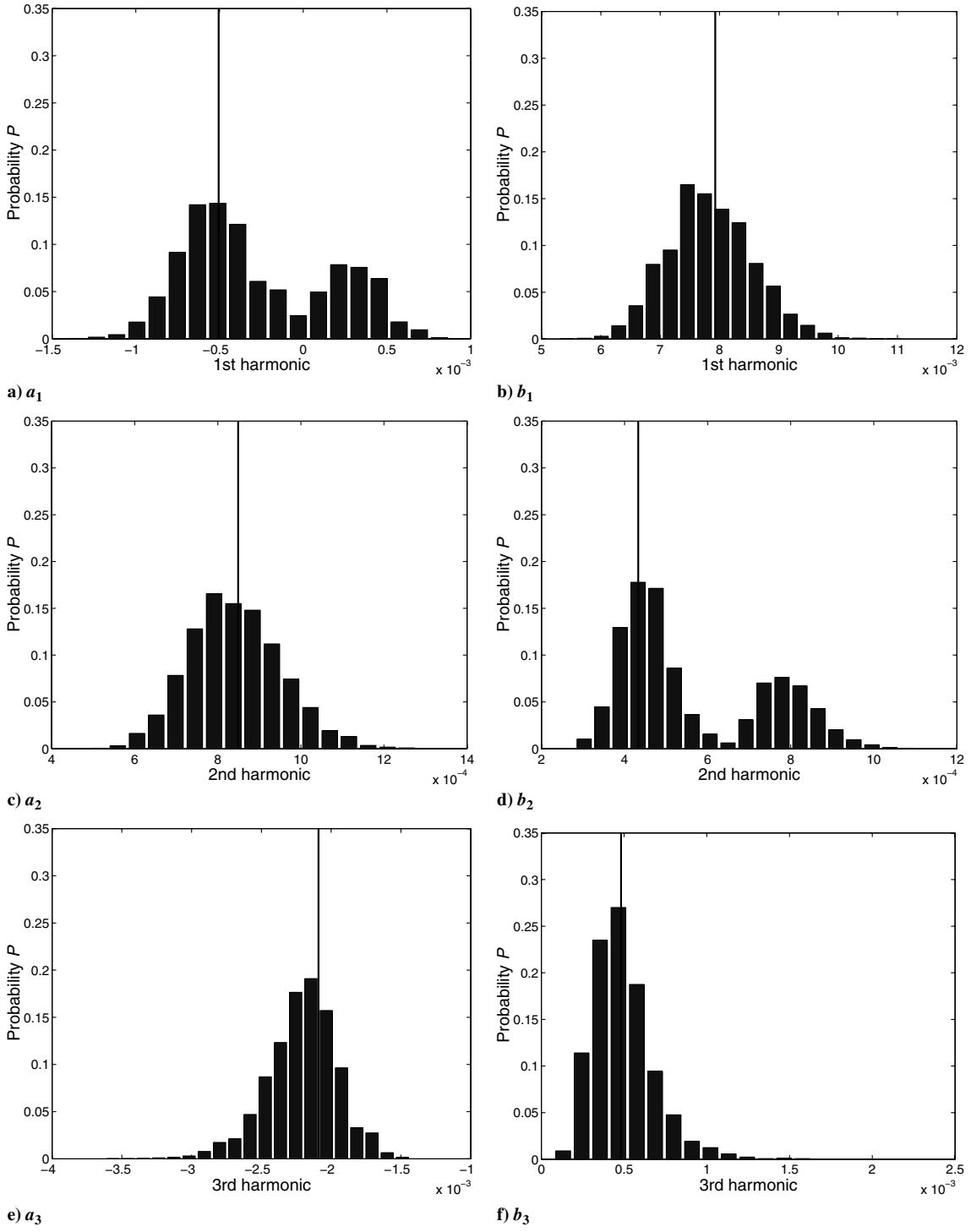

Fig. 27 Probability histogram of first three harmonics of the blade-tip torsional response (solid line is the baseline value).

in the material properties. Finally, the effect of uncertainty on vibratory hub loads and stability can be evaluated. These issues are subjects of future work.

Conclusions

The aeroelastic response of a composite helicopter rotor with material uncertainty is studied. The composite material properties E_1, E_2, G_{12}, and ν_{12} are modeled as independent, normally distributed, random variables. The effect of material uncertainties on the cross-sectional stiffness, nonrotating and rotating natural frequencies, and aeroelastic response of the composite rotor blade are evaluated using Monte Carlo simulations. The following conclusions are drawn from this study:

1) The flap, lag, and torsional stiffnesses of the composite rotor blade show c.o.v. of 6.14, 6.14, and 5.60%, respectively, when uncertainty is considered in the material properties.

2) The flap, lag, and torsional fundamental natural frequencies of the nonrotating composite blade, as expected, show c.o.v. of 3.07, 3.07, and 2.80%, respectively. The higher mode frequencies of flap, lag, and torsion show the same c.o.v. as their respective fundamental frequencies. This result, though trivial, serves to additionally validate the convergence after 6000 MCS.

3) The flap, lag, and torsional fundamental natural frequencies of the rotating composite blade show c.o.v. of 0.35, 2.06, and 1.26%,

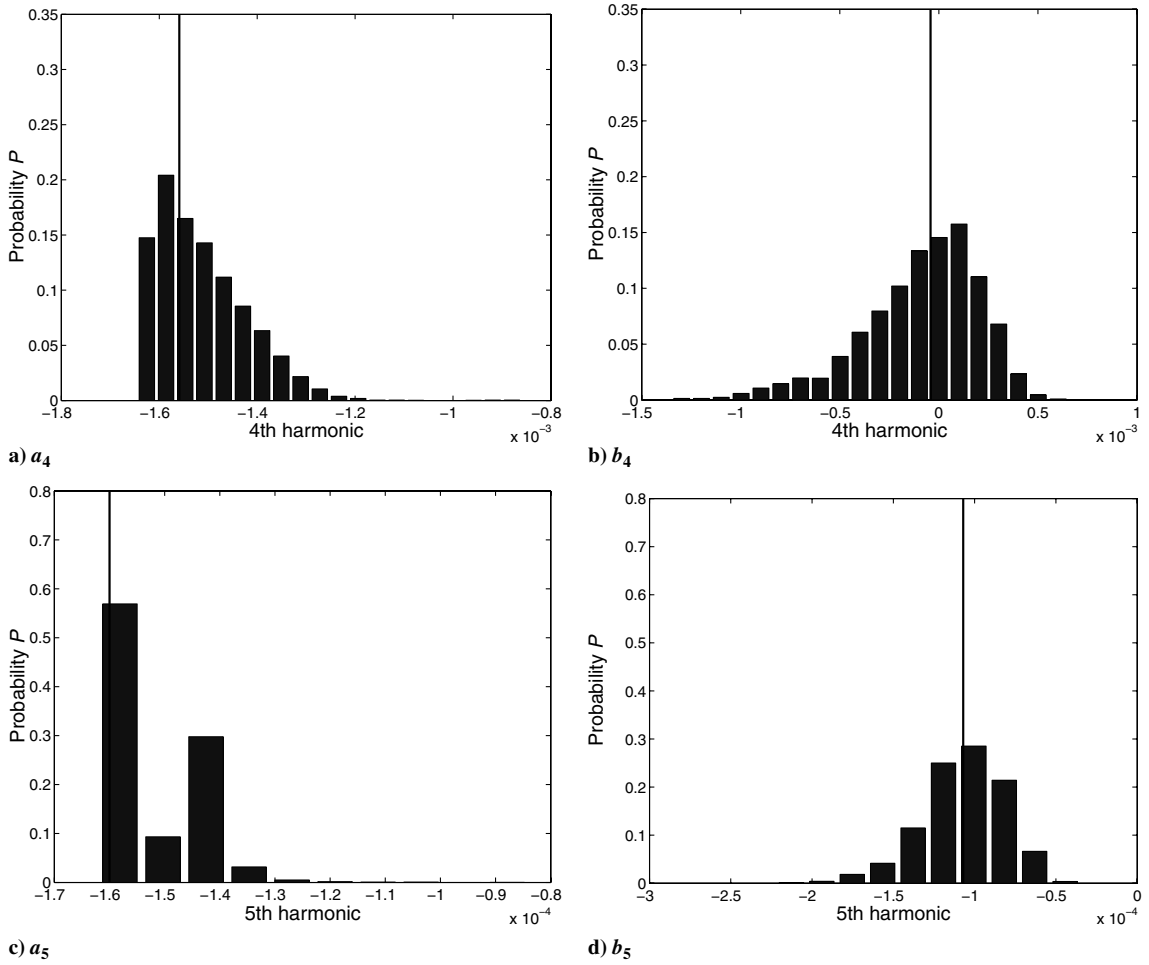

Fig. 28 Probability histogram of fourth and fifth harmonics of the blade-tip torsional response (solid line is the baseline value).

respectively. The flap natural frequencies are less sensitive to material uncertainty than the lag and torsional frequencies. The rotating blade shows comparatively less c.o.v. than the nonrotating blade because of centrifugal stiffening. Also, the c.o.v. of the rotating blade natural frequencies vary with modes because of the relative importance of structural stiffness vis-a-vis the centrifugal stiffness.

4) The aeroelastic response of the composite helicopter rotor shows a considerable deviation from the baseline value response due to material uncertainty. The probability distribution of the blade-tip response varies along the azimuth because of the structural and aerodynamic interactions. Also, the Fourier coefficients of the blade response suffer considerable impact of the material uncertainty.

5) The deviation in the aeroelastic response affects accurate prediction of performance parameters, vibratory loads, and aeroelastic stability of the rotorcraft. Therefore, aeroelastic design of rotorcraft should consider the randomness in composite material properties.

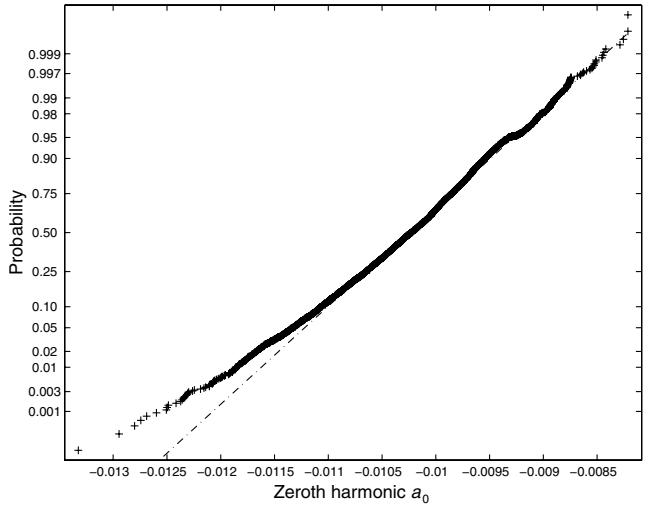

Fig. 29 Normal probability plot of torsional response of zeroth harmonic a_0.

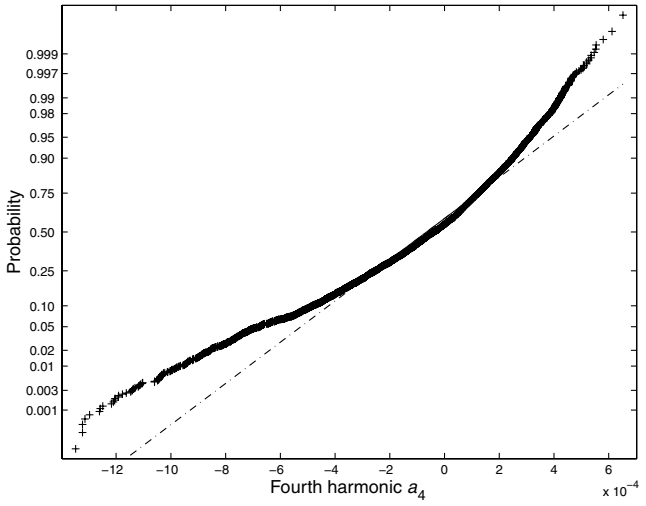

Fig. 30 Normal probability plot of torsional response of fourth harmonic a_4.

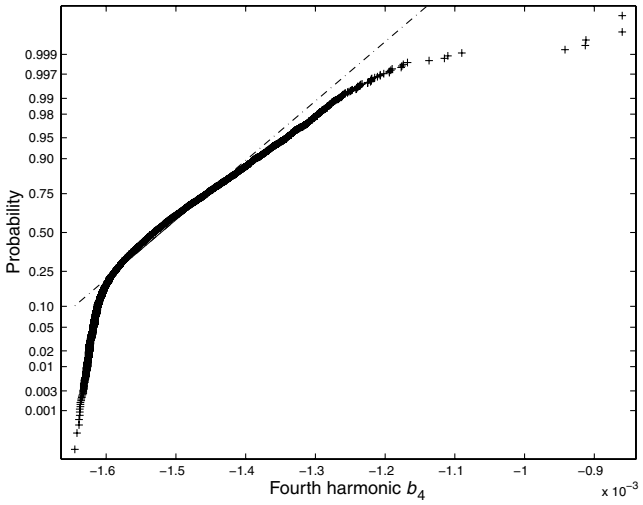

Fig. 31 Normal probability plot of torsional response of fourth harmonic b_4.

Appendix: Structural and Centrifugal Strain Energy Terms

The rotating frequency calculations of the composite blade uses the following key strain energy terms for the lag v, flap w, and torsion ϕ motions, which are decoupled for the simple configuration considered:

$$
\begin{aligned}
2U_v &= \underbrace{\int_0^R EI_z \times (v'')^2 \,\mathrm{d}x}_{\text{nonrotating part}} + \underbrace{\int_0^R [F_A \times (v')^2 - m\Omega^2 v^2] \,\mathrm{d}x}_{\text{rotating part}} \\
2U_w &= \underbrace{\int_0^R EI_y \times (w'')^2 \,\mathrm{d}x}_{\text{nonrotating part}} + \underbrace{\int_0^R [F_A \times (w')^2] \,\mathrm{d}x}_{\text{rotating part}} \\
2U_\phi &= \underbrace{\int_0^R GJ \times (\phi')^2 \,\mathrm{d}x}_{\text{nonrotating part}} + \underbrace{\int_0^R [m\Omega^2 (k_{m2}^2 - k_{m1}^2)\phi^2] \,\mathrm{d}x}_{\text{rotating part}}
\end{aligned}
\tag{A1}
$$

where R is the radius of the blade, F_A is the blade axial force, and k_{m1} and k_{m2} are the blade cross-sectional radii of gyration in the flap and lag directions, respectively.

References

[1] Vinckenroy, G. V., and Wilde, W. P. De., "The Use of Monte Carlo Techniques in Statistical Finite Element Methods for the Determination of the Structural Behaviour of Composite Materials Structural Components," *Composite Structures*, Vol. 32, Nos. 1–4, 1995, pp. 247–253. doi:10.1016/0263-8223(95)00055-0

[2] Singh, B. N., Yadav, D., and Iyengar, N. G. R., "Free Vibration of Composite Cylindrical Panels with Random Material Properties," *Composite Structures*, Vol. 58, No. 4, 2002, pp. 435–442. doi:10.1016/S0263-8223(02)00133-2

[3] Salim, S., Yadav, D., and Iyengar, N. G. R., "Analysis of Composite Plates with Random Material Characteristics," *Mechanics Research Communications*, Vol. 20, No. 5, 1993, pp. 405–414. doi:10.1016/0093-6413(93)90031-I

[4] Yadav, D., and Verma, N., "Buckling of Composite Circular Cylindrical Shells with Random Material Properties," *Composite Structures*, Vol. 37, Nos. 3–4, 1997, pp. 385–391. doi:10.1016/S0263-8223(97)00032-9

[5] Onkar, A. K., and Yadav, D., "Forced Nonlinear Vibration of Laminated Composite Plates with Random Material Properties," *Composite Structures*, Vol. 70, No. 3, 2005, pp. 334–342. doi:10.1016/j.compstruct.2004.08.037

[6] Onkar, A. K., and Yadav, D., "Non-linear Response Statistics of Composite Laminates with Random Material Properties under Random Loading," *Composite Structures*, Vol. 60, No. 4, 2003, pp. 375–383. doi:10.1016/S0263-8223(03)00049-7

[7] Pettit, C. L., and Beran, P. S., "Effects of Parametric Uncertainty on Airfoil Limit Cycle Oscillation," *Journal of Aircraft*, Vol. 40, No. 5, 2003, pp. 1004–1006.

[8] Lindsley, N. J., Beran, P. S., and Pettit, C. L., "Effects of Uncertainty on Nonlinear Plate Aeroelastic Response," AIAA Paper 2002-1271, 22–25 April 2002.

[9] Peter, J. A., and Dowell, E. H., "Stochastic Analysis of a Nonlinear Aeroelastic Model using the Response Surface Method," *Journal of Aircraft*, Vol. 43, No. 4, 2006, pp. 1044–1052. doi:10.2514/1.17525

[10] Pettit, C. L., "Uncertainty Quantification in Aeroelasticity: Recent Results and Research Challenges," *Journal of Aircraft*, Vol. 41, No. 5, 2004, pp. 1217–1229.

[11] Kim, T. K., and Hwang, I. H., "Reliability Analysis of Composite Wing Subjected to Gust Loads," *Composite Structures*, Vol. 66, Nos. 1–4, 2004, pp. 527–531. doi:10.1016/j.compstruct.2004.04.072

[12] Pradlwarter, H. J., Pellissetti, M. F., Schenk, C. A., Schuëller, G. I., Kreis, A., Fransen, S., Calvi, A., and Klein, M., "Realistic and Efficient Reliability Estimation for Aerospace Structures," *Computer Methods in Applied Mechanics and Engineering*, Vol. 194, Nos. 12–16, 2005, pp. 1597–1617. doi:10.1016/j.cma.2004.05.029

[13] Koutsourelakis, P. S., Kuntiyawichai, K., and Schuëller, G. I., "Effect of Material Uncertainties on Fatigue Life Calculations of Aircraft Fuselages: A Cohesive Element Model," *Engineering Fracture Mechanics*, Vol. 73, No. 9, 2006, pp. 1202–1219. doi:10.1016/j.engfracmech.2006.01.003

[14] Smith, E. C., and Chopra, I., "Aeroelastic Response, Loads, and Stability of a Composite Rotor in Forward Flight," *AIAA Journal*, Vol. 31, No. 7, 1993, pp. 1265–1273.

[15] Volovoi, V., Hodges, D. H., Cesnik, C., and Popescu, B., "Assessment of Beam Modeling for Rotor Blade Application," *Mathematical and Computer Modelling*, Vol. 33, Nos. 10–11, 2001, pp. 1099–1112. doi:10.1016/S0895-7177(00)00302-2

[16] Friedmann, P. P., "Rotary-Wing Aeroelasticity: Current Status and Future Trends," *AIAA Journal*, Vol. 42, No. 10, 2004, pp. 1953–1972.

[17] Ganguli, R., "A Survey of Recent Developments in Rotorcraft Design Optimization," *Journal of Aircraft*, Vol. 41, No. 3, 2004, pp. 493–510.

[18] Pawar, P. M., and Ganguli, R., "On the Effect of Progressive Damage on Composite Helicopter Rotor System Behavior," *Composite Structures*, Vol. 78, No. 3, 2007, pp. 410–423. doi:10.1016/j.compstruct.2005.11.043

[19] Friedmann, P. P., and Hodges, D. H., "Rotary Wing Aeroelasticity—A Historical Perspective," *Journal of Aircraft*, Vol. 40, No. 6, 2003, pp. 1019–1046.

[20] Elishakoff, I., *Probabilistic Methods in the Theory of Structures*, Wiley, New York, 1983.

[21] Kleiber, M., and Hien, T. D., *The Stochastic Finite Element Method, Basic Perturbation Technique and Computer Implementation*, Wiley, New York, 1992.

[22] Lutes, L. D., and Sarkani, S., *Stochastic Analysis of Structural and Mechanical Vibrations*, Prentice–Hall, Upper Saddle River, NJ, 1997.

[23] Ishida, R., "Stochastic Finite Element Analysis of Beam with Statistical Uncertainties," *AIAA Journal*, Vol. 39, No. 11, 2001, pp. 2192–2197.

[24] Kunz, D., "Comprehensive Rotorcraft Analysis: Past, Present, and Future,"46th AIAA/ASME/ASCE/AHS/ASC Structures, Structural Dynamics and Materials Conference, Austin, TX, AIAA Paper 2009-2244, Apr. 2005.

[25] Jung, S. N., Nagaraj, V. T., and Chopra, I., "Refined Structural Dynamics Model for Composite Rotor Blades," *AIAA Journal*, Vol. 39, No. 2, 2001, pp. 339–348.

[26] Cesnik, C. E. S., and Hodges, D. H., "VABS: A New Concept for Composite Rotor Blade Cross-Sectional Modeling," *Journal of the American Helicopter Society*, Vol. 42, No. 1, 1997, pp. 27–38.

[27] Smith, E. C., and Chopra, I., "Formulation and Evaluation of an Analytical Model for Composite Box-Beams," *Journal of the American Helicopter Society*, Vol. 36, No. 3, 1991, pp. 23–35.

[28] Ganguli, R., and Chopra, I., "Aeroelastic Optimization of a Helicopter Rotor to Minimize Vibration and Dynamic Stresses," *Journal of Aircraft*, Vol. 12, No. 4, 1996, pp. 808–815.

[29] Murugan, M. S., Suresh, N., Ganguli, R., and Mani, V., "Target Vector Optimization of Composite Box-Beam Using Real Coded Genetic Algorithm: A Decomposition Approach," *Structural and Multidisciplinary Optimization*, Vol. 33, No. 2, 2007, pp. 131–146. doi:10.1007/s00158-006-0030-1

[30] Bir, G., Chopra, I., and Ganguli, R., "University of Maryland Advanced Rotorcraft Code (UMARC) Theory Manual," UM-AERO Rept. 92-02, Univ. of Maryland, College Park, MD, 1992.

[31] Borri, M., "Helicopter Rotor Dynamics by Finite Element Time Approximation," *Computers and Mathematics with Applications (1975-) / Computers & Mathematics with Applications*, Vol. 12, No. 1, 1986, pp. 149–160. doi:10.1016/0898-1221(86)90092-1

[32] Hansford, R. E., "A Unified Formulation of Rotor Loads Prediction Methods," *Journal of the American Helicopter Society*, Vol. 31, No. 2, 1986, pp. 58–65.

[33] Ganguli, R., "Optimum Design of a Helicopter Rotor for Low Vibration using Aeroelastic Analysis and Response Surface Methods," *Journal of Sound and Vibration*, Vol. 258, No. 2, 2002, pp. 327–344. doi:10.1006/jsvi.2002.5179

[34] Murugan, M. S., and Ganguli, R., "Aeroelastic Stability Enhancement and Vibration Suppression in a Composite Helicopter Rotor," *Journal of Aircraft*, Vol. 42, No. 4, 2005, pp. 1013–1024.

[35] Johnson, W., *Helicopter Theory*, Princeton Univ. Press, Princeton, NJ, 1980.

[36] Ganguli, R., Chopra, I., and Weller, W. H., "Comparison of Calculated Vibratory Rotor Hub Loads with Experimental Data," *Journal of the American Helicopter Society*, Vol. 43, No. 4, 1998, pp. 312–318.

[37] Hansford, R. E., and Vorwald, J., "Dynamics Workshop on Rotor Vibratory Loads Prediction," *Journal of the American Helicopter Society*, Vol. 43, No. 1, 1998, pp. 76–87.

[38] Yeo, H., and Johnson, W., "Assessment of Comprehensive Analysis Calculation of Airloads on Helicopter Rotors," *Journal of Aircraft*, Vol. 42, No. 5, 2005, pp. 1218–1228.

[39] Datta, A., Sitaraman, J., Chopra, I., and Baeder, J. D., "CFD/CSD Prediction of Rotor Vibratory Loads in High-Speed Flight," *Journal of Aircraft*, Vol. 43, No. 6, 2006, pp. 1698–1709.